9-16-2013

The Role Of Microstructure Refinement On The Impact Ignition And Combustion Behavior Of Mechanically Activated Ni/Al Reactive Composites

B A. Mason
Purdue University, bamason@purdue.edu

Lori J. Groven
Purdue University

Steven F. Son
Purdue Univer

Recommended Citation
B. A. Mason, L. J. Groven, and S. F. Son, "The Role of Microstructure Refinement on the Impact Ignition and Combustion Behavior of Mechanically Activated Ni/Al Reactive Composites," Journal of Applied Physics, Vol. 114(11), p. 113501 (2013). dx.doi.org/10.1063/1.4821236

The role of microstructure refinement on the impact ignition and combustion behavior of mechanically activated Ni/Al reactive composites

B. A. Mason, L. J. Groven, and S. F. Son

Citation: Journal of Applied Physics **114**, 113501 (2013);
View online: https://doi.org/10.1063/1.4821236
View Table of Contents: http://aip.scitation.org/toc/jap/114/11
Published by the American Institute of Physics

JOURNAL OF APPLIED PHYSICS **114**, 113501 (2013)

The role of microstructure refinement on the impact ignition and combustion behavior of mechanically activated Ni/Al reactive composites

B. A. Mason,[a] L. J. Groven, and S. F. Son
School of Mechanical Engineering, Purdue University, West Lafayette, Indiana 47907, USA

(Received 2 July 2013; accepted 29 August 2013; published online 16 September 2013)

Metal-based reactive composites have great potential as energetic materials due to their high energy densities and potential uses as structural energetic materials and enhanced blast materials however these materials can be difficult to ignite with typical particle size ranges. Recent work has shown that mechanical activation of reactive powders increases their ignition sensitivity, yet it is not fully understood how the role of microstructure refinement due to the duration of mechanical activation will influence the impact ignition and combustion behavior of these materials. In this work, impact ignition and combustion behavior of compacted mechanically activated Ni/Al reactive powder were studied using a modified Asay shear impact experiment where properties such as the impact ignition threshold, ignition delay time, and combustion velocity were identified as a function of milling time. It was found that the mechanical impact ignition threshold decreases from an impact energy of greater than 500 J to an impact energy of ~50 J as the dry milling time increases. The largest jump in sensitivity was between the dry milling times of 25% of critical reaction milling time (t_{cr}) (4.25 min) and 50% t_{cr} (8.5 min) corresponding to the time at which nanolaminate structures begin to form during the mechanical activation process. Differential scanning calorimetry analysis indicates that this jump in the sensitivity to thermal and mechanical impact is dictated by the formation of nanolaminate structures, which reduce the temperature needed to begin the dissolution of nickel into aluminum. It was shown that a milling time of 50%–75% t_{cr} may be near optimal when taking into account both the increased ignition sensitivity of mechanical activated Ni/Al and potential loss in reaction energy for longer milling times. Ignition delays due to the formation of hotspots ranged from 1.2 to 6.5 ms and were observed to be in the same range for all milling times considered less than t_{cr}. Combustion velocities ranged from 20–23 cm/s for thermally ignited samples and from 25–31 cm/s for impacted samples at an impact energy of 200–250 J.
 [http://dx.doi.org/10.1063/1.4821236]

I. INTRODUCTION

Metal-based reactive powder composites, such as Ni/Al, are a class of energetic materials that have high-energy densities and can produce significant energy output during reaction by thermal or mechanical initiation. Their potential use as structural energetic materials, as enhanced blast materials and for the synthesis of novel metastable non-equilibrium materials has driven research focused on their mechanical impact behavior.[1–3] Numerous experimental and theoretical studies have been published on impact behavior and shock compression of metal-based reactive powder mixtures with metals such as Al, Ni, Si, Ti, W, Nb, and more.[1–5] Yet the fundamental mechanisms that govern the initiation and front propagation are not well understood. For example, their energy release characteristics depend on the mode of initiation, and reaction propagation, in a currently unpredictable way. The lack of a predictive understanding of these materials leads to their underutilization and therefore significant effort is being dedicated to characterizing and modeling these reactions.[1]

Two distinct modes for reaction upon impact have been identified, shock-assisted and shock-induced chemical reactions.[6] Shock-assisted reactions occur in the period of thermal equilibration typically well after the shock wave has passed. In contrast, shock-induced reactions occur within or immediately after the pressure rise of the shockwave upon mechanical impact. Shock-assisted reactions occur due to heat generation from the compaction of the reactive material. This mechanical heating can be caused by plastic deformation, pore collapse, brittle fracture of particles, friction between particles, and shockwave interactions. Chemical reaction occurs following this mechanical dissipative heating. This reaction may continue and transition to a combustion wave, or quench.

In the regime of shock-assisted reactions, it has been shown that most metal-based reactive composites, such as Ni/Al, require high impact energies in order to initiate a reaction.[1,7] However, nanoscale reactive composites are significantly more sensitive to impact and thermal ignition and have faster reaction rates than mixtures using micron size powders due to higher surface areas and smaller diffusion distances.[2,8,9] It has also been observed that higher bulk densities can lower impact ignition thresholds in nano mixtures.[2] In addition, material properties such as ductility and yield strength will also play a large role. For example, when the

[a]Author to whom correspondence should be addressed. Electronic mail: bamason@purdue.edu

reactive composite W/Al is impacted, the ignition threshold is lower than that of Ni/Al. It was theorized that the lower ignition threshold of W/Al is due to the harder material (W) slicing through the more ductile material (Al) upon impact creating fresh interfaces and igniting the sample.[2] Therefore, for the W/Al reactive composite, the energy needed to initiate reaction is acquired through both mechanical and thermal means; whereas for the Ni/Al reactive composite, the energy needed to initiate reaction is acquired mainly through thermal build up during the impact.

In addition to nanopowders, arrested reactive milling (ARM) or mechanical activation (MA) performed by high energy ball milling has been used to decrease the impact ignition of these materials.[4,5,10] Increasing the ignition sensitivities through MA occurs by changes in morphology, ductility, and hardness through cold working. This is achieved by high energy collisions between the particles and milling media. When milling is arrested before the critical reaction time of a reactive mixture, such as Ni/Al, composite particles are produced that consist of intermixed material with structures/laminates on the micron to nanoscale. It has been shown that the intermixing of these materials on an intimate scale causes the observed increase in thermal and impact sensitivity due to smaller diffusion distances.[5,10–14] However, the role and extent to which the modified microstructure properties have on compaction, ignition, and subsequent reaction propagation of impacted reactive powders has yet to be fully investigated and quantified.

A recent impact study using a rod-on-anvil Taylor impact test setup and small cylindrical samples of MA Ni/Al have indicated that milling duration affects ignition thresholds.[5] It was observed that material milled for 35% of the critical milling time (t_{cr}) had lower impact ignition thresholds than material milled for 65% t_{cr}, where the t_{cr} is the time at which reaction of the Ni/Al material would take place during milling if the milling is not arrested first. It was stated that this behavior is a result of competing effects of increased reactivity and increased strain hardening as the duration of milling increases.[5] This work, however, only investigated two milling durations and did not investigate combustion behavior upon reaction and therefore further work is required.

The objective of this work is to gain a better understanding of how the variation of microstructure, modified via milling parameters, influences the impact ignition and reaction propagation behavior of MA Ni/Al. With this information, a more comprehensive understanding can be gained along with data that can be used to validate and calibrate continuum and molecular dynamic models that are currently being developed in conjunction with this work.[15,16]

II. EXPERIMENTAL

A. Mechanical activation and powder characteristics

For this study, 3–7 μm Ni (Alfa Aesar) and −325 mesh Al (Alfa Aesar) were used to prepare an equiatomic MA Ni/Al reactive composite powder using a two-step dry and wet milling procedure as detailed in previous work.[10] In short, the Ni/Al was milled by high energy ball milling in a pure argon atmosphere using a PM100 (Retsch, Germany) planetary ball mill. The reactant powders were subjected to dry milling for different time durations that include 0, 4.25, 8.5, 12.75, and 17 min corresponding with roughly 0%, 25%, 75%, and 97% of the critical milling time (t_{cr}) (when exothermic reaction occurs). After dry milling, the material was milled with hexane (98.5% hexane isomers, Mallinckrodt Chemicals) for a total of 10 min and then dried as previously reported.[10]

Characterization of the resulting MA reactive composite powder was done by scanning electron microscopy (SEM), energy dispersive spectroscopy (EDS), scanning transmission electron microscopy (STEM), and X-ray diffraction (XRD). Full details of this characterization can be found in Ref. 10. In summary, the milled Ni/Al powder consists of composite particles of intermixed Ni/Al having both course and fine microstructures. The course microstructure consists of Ni and Al intermixing with features on the micron-scale. Whereas, the material consisting of the fine microstructure consists of Ni and Al nanolaminate layers that are less than 30 nm thick. Materials dry milled for 25% t_{cr} (4.25 min), or less, consist primarily of course microstructure, materials dry milled for 50% and 75% t_{cr} have a mixture of course and nanolaminate microstructures to varying degrees depending upon milling time and particle size. Material dry milled for 97% t_{cr} consists of primarily the nanolaminate microstructure.

In this work, further characterization has been conducted to determine the heats of reaction of the MA Ni/Al as a function of milling time. This was done with a TA Instruments Q600 simultaneous thermo gravimetric analyzer and differential scanning calorimeter (TGA/DSC). In each experiment, ~20 mg of reactive material was heated at a heating rate of 10 K/min in an atmosphere of 99.9998% pure argon with flow rate of 100 cm^3/min to 800 K.

B. Impact experiments

Reaction initiation by mechanical impact was accomplished using the Asay shear experiment used previously with explosives[17] and other Ni/Al impact studies.[9,10,12,18] The schematic of the experiments is show in Fig. 1. For these experiments, MA Ni/Al power with a sieved particle size range of $25 < d < 53$ μm was compacted into square samples with nominal dimensions of 20 mm × 20 mm × 2 mm by applying a uniaxial pressure of 670 MPa. A particle size

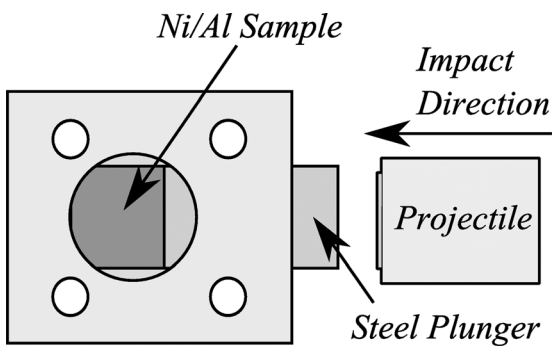

FIG. 1. Diagram of Asay shear impact experiment using a flat plunger with the windowed sample holder.

range of $25 < d < 53\ \mu m$ was used. The compacts were pressed to a stop and a relative density in the range of 68%–72% TMD was achieved. The compacted samples were placed into a specially designed holder equipped with an acrylic window for imaging the sample during the impact and subsequent reaction. A steel flyer plate press fit into a Delrin projectile (24 g in total mass and 25.4 mm diameter) was accelerated by means of a gas gun at a set velocity in the range of 50–220 m/s or an impact energy of 30–600 J. The impact energy is simply the standard kinetic energy of the Delrin projectile. The projectile impacts a plunger inserted into a slot on the side of the sample holder. The plungers used had a flat impact face and had the same thickness and height of the MA Ni/Al compact. Impact experiments were recorded using a Phantom 7.3 high-speed camera at 50 000–88 000 fps.

In addition to impact experiments, samples were also thermally ignited. Pressed samples were placed in the impact holder to maintain similar heat loss condition as the impact experiments. The samples were ignited with Nichrome wire with an ignition increment of ~75 mg of loose MA Ni/Al powder placed on top of the sample. Burning rates were measured with a Phantom 7.3 high-speed camera at 3000 fps.

III. RESULTS AND DISCUSSION

The role of microstructure refinement on the mechanical impact ignition thresholds or the combustion characteristics after impact is not fully understood. Using a simple particle ignition experiment,[10] it was previously reported that MA Ni/Al can have thermal ignition thresholds of less than 650 K and that by increasing the amount of dry milling the thermal ignition threshold can be reduced slightly from 650 K to 550 K for sieved $25 < d < 53\ \mu m$ material. Whereas, the thermal ignition threshold of non-milled, micron-size, Ni/Al is typically very close to the eutectic temperature of the system (~912 K).[19–22] Therefore, it is expected that the impact ignition thresholds for shock-assisted reactions in the MA Ni/Al will also decrease as a function of dry milling time with the most sensitive material being dry milled for 97% t_{cr}.

A. Impact ignition thresholds

To investigate how the impact ignition thresholds of shock-assisted reactions in MA Ni/Al are related to dry milling time and the thermal ignition thresholds, the MA Ni/Al material having a particle size of $25 < d < 53\ \mu m$ size was impacted as a function of milling time and impact energy. Figure 2 summarizes the experimental results as a function of dry milling time and impact energy on a "Go," "No-go" basis ("Go" for a reaction ignition and "No-go" for no ignition). The ignition threshold was found to be between 160–200 J (115–130 m/s) for material dry milled for 50% t_{cr} and the lowest ignition threshold was identified to be between 40–60 J (60–70 m/s) for material dry milled at 97% t_{cr}. The impact thresholds for MA Ni/Al milled for 25% t_{cr} or less (including samples with no MA) could not be found as they did not react for the range of impact energies considered, even at the maximum experimental projectile speed of ~200 m/s (500 J). These results show that the

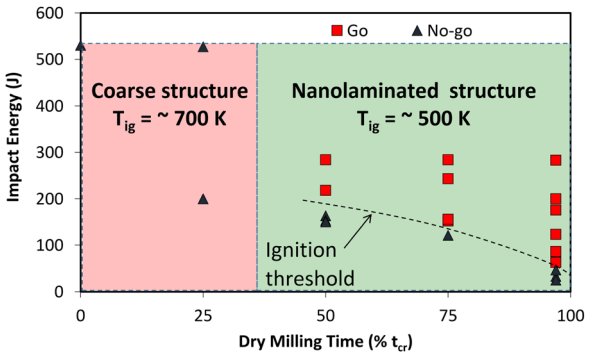

FIG. 2. Impact reaction thresholds as a function of milling time and impact energy for compacts having initial particle size of $25 < d < 53\ \mu m$.

impact ignition threshold decreases significantly between dry milling times of 25% t_{cr} and 50% t_{cr}, corresponding to the appearance of nanolaminate microstructure. At milling times greater than 50% t_{cr}, the impact ignition threshold continues to decrease but more moderately, following a similar trend as the thermal ignition thresholds previously published.[10] This indicates that the sensitivity to impact ignition is directly correlated to the fraction of nanolaminate structure within the MA Ni/Al reactive composite, with the largest increase in sensitivity occurring with the initial formation of nanolaminate intra-particle microstructure.

These results are quite different than those reported by Herbold *et al.*[5] which showed a minimum ignition threshold for shorter milling durations (35% t_{cr}). These differences can be attributed to the type of impact experiment performed and the method of mechanical activation. The samples were impacted were using a rod-on-anvil Taylor impact experimental setup where the sample was unconfined resulting in rapid plastic deformation and then dispersion of the sample into the ambient environment. It was stated that rapid plastic deformation of the particles was the driving force that produced mechanical heating upon impact leading to ignition, which is why the material milled at 35% t_{cr} had a lower impact threshold than the material milled at 65% t_{cr} as the material milled for 35% t_{cr} was expected to be more ductile. However, hardness measurements were not reported. In our work, the samples were confined during impact preventing particles from dispersing into the ambient environment. This configuration allows for heat generation over an extended time and the observation of delayed reactions. As a result, sample ignition can be caused by heating during (e.g., plastic deformation) and after the impact (e.g., heating due to shock wave reflections or localized hot spot ignition). Differences in mechanical activation may also explain the observed differences as the properties of the MA of Ni/Al material will vary not only due to milling duration but also to other parameters such as, but not limited to, initial particle size, type of mill, and charge ratio. It has been shown that varying milling parameters such as the initial powder size, and the charge ratio results in significant differences in the resulting microstructure[11,23,24] such as the Ni/Al laminate frequency and size, which will affect properties such as the material's ductility, heat of reaction, and will in-turn inevitably affect the impact ignition sensitivity.

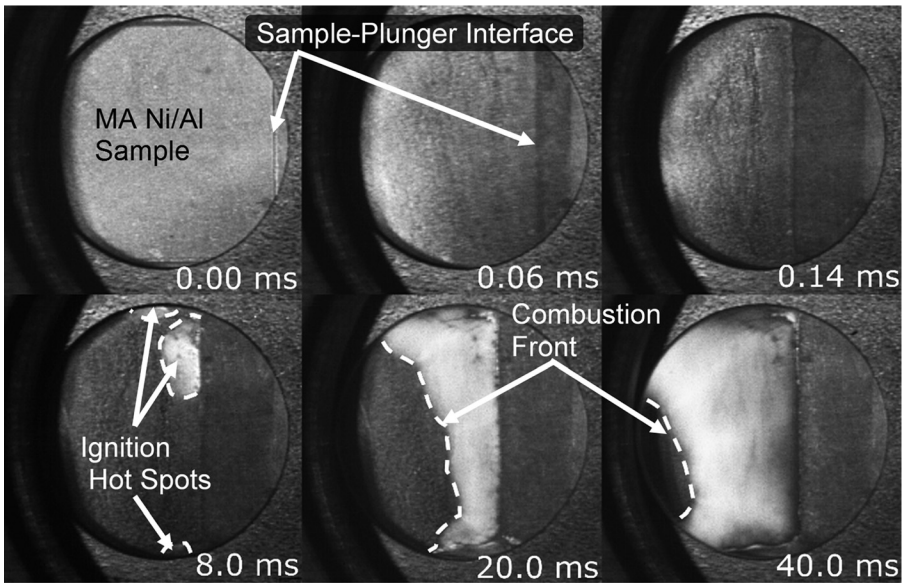

FIG. 3. Impact ignition and reaction of MA Ni/Al compacts using a flat plunger.

B. Hotspot ignition

In a typical impact experiment at projectile velocities of 50–150 m/s, the plunger impacts the Ni/Al sample at an initial velocity of 35–100 m/s, respectively. This results in an impact energy of 30–280 J and a lateral displacement of the plunger by about 4–9 mm depending upon the impact velocity. Still images of a typical impact and subsequent reactions are shown in Fig. 3 for the flat plunger cases. The first three images show the flat plunger impacting a MA Ni/Al sample with an impact energy of about 200 J (130 m/s projectile velocity). The total time of compaction was 0.14 ms. The third image at $t = 8$ ms shows the sample about 3 ms after the sample initially ignited, where $t = 0$ is the time at which the plunger is observed to begin to move. In this frame, 3 of 4 ignition locations or hotspots are visible. The first luminescent hotspot appeared at about $t = 5.4$ ms followed by ignition of other hotspots at various locations, the last of which ignited at $t = 11.2$ ms. The combustion front propagation (right to left) is seen at times $t = 20$ ms and $t = 40$ ms in the last two images of Fig. 3. The hotspot ignition was identified by the commencement of a luminous combustion front from a specific point. It was observed that for impact experiments using the flat plunger, ignition typically occurred by hotspot formation in 2–5 locations at the plunger-sample interface, along the upper and lower edges of the compact and occasionally within the bulk of the sample.

The ignition delays, defined by the time at which the *first* luminous hotspot appeared after impact that was followed by combustion propagation, are show in Fig. 4. The ignition delays for MA Ni/Al compacts impacted at impact energies of 200–250 J (projectile velocities of 130–145 m/s) ranged from about 1.2 to 6.5 ms. In Table I, hotspot ignition times for each hotspot observed during an experiment are shown for 2–3 samples for each milling time. The hotspot ignition delays ranged from about 1.2 to 15 ms.

All the samples were impacted at roughly the same conditions and therefore the heat generation upon impact is very similar for each case. Consequently, it could be expected that the samples with higher thermal ignition thresholds (i.e., shorter milling times) would have longer ignition delays due to the length of time that is required for the temperature to reach the thermal ignition threshold temperature after impact. However, this trend was not clearly observed. The results do show that the earliest ignition delay was measured for a sample dry milled for 97% t_{cr}, followed by 75% t_{cr}, and then 50% t_{cr}. However, the longest ignition delays were also measured for the material milled for 97% t_{cr}. It appears that the ignition delays are not strongly dependent upon milling time as long as the material is milled for at least 50% t_{cr} and that the variability in ignition delays observed is simply the intrinsic variability of the experiment. The variability does seem to increase as the critical milling time is reached, but the reason for that is unclear.

C. Combustion velocities

As previously shown in Fig. 3, upon ignition, the reaction fronts were seen to propagate through the sample originating from the hotspot locations. Based on the

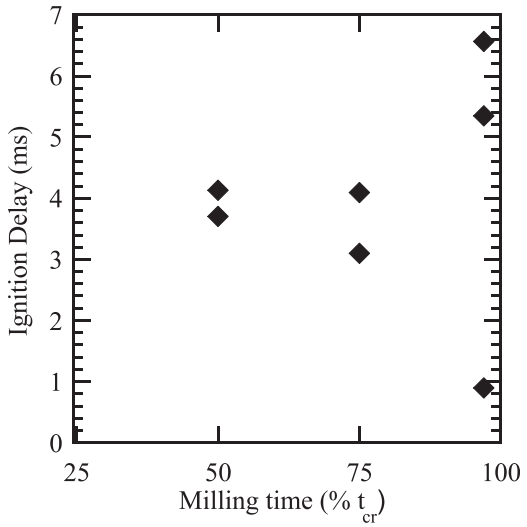

FIG. 4. Ignition delay times for MA Ni/Al samples impacted at with an impact energy of 200–250 J (130–145 m/s).

TABLE I. Hotspot ignition delay times for MA Ni/Al samples as a function of milling time that were impacted at with an impact energy of 200–250 J (130–145 m/s). Each impact experiment exhibits 2-5 hotspot ignition points.

	Hotspot ignition times (ms)		
Sample	50% t_{cr}	75% t_{cr}	97% t_{cr}
1	3.7, 3.8, 3.9, 4.5	3.1, 4.1, 7.0, 8.8, 9.4	6.5, 10.6, 12.6
2	4.1, 10.7	4.1, 11.1, 8.6, 8.8	1.2, 5.0, 15.5
3			5.4, 6.7, 7.1, 11.16

microstructure characterization, it might be expected that combustion velocities would increase as a function of milling time due to an increased concentration of nanolaminate microstructure (decrease in diffusion distances) and lower reaction thresholds,[10] however this was not observed. For both thermally and impact ignited cases, the combustion velocities did not vary significantly as a function of dry milling time for those considered. It should be noted that Ni/Al with no MA at 70% TMD would not ignite without substantial preheating, nor would it ignite upon impact for the impact energies considered. For MA Ni/Al compacts thermally ignited within the sample holder, the average combustion velocities were measured to be between 21–23 cm/s (see Fig. 5). In comparison, combustion velocities ranged from 25–31 cm/s for samples impacted with at an impact energy of 200–250 J. In Fig. 5, the average combustion velocity and the range of velocities observed are reported. The increase in combustion velocity for the impacted samples as compared to the thermally ignited samples is due to a higher packing density and to an increased initial temperature as a result of the impact. Both of these conditions have been shown to increase the combustion velocity of the Ni/Al reaction.[4,25]

The observed combustion velocities are also much faster than previously reported for both milled and unmilled Ni/Al reactives with micron sized powders. Taking into account both loose powder mixtures and cold-pressed compacts, typical combustion velocities have been reported to be on the order of 1–12 cm/s.[4,26] Recently, Bacciochini *et al.*[4] reported combustion velocities for thermally ignited MA Ni/Al compacts cold-pressed to 40%–80% TMD in the range of 3–6 cm/s. The combustion velocities in this work are 4–10 × faster than those. However, the milling procedure utilized by Bacciochini *et al.*[4] varied significantly from that of this work. In their work, the critical dry milling time was between 38–42 min, whereas the critical milling time for this work is between 17–17.5 min. Therefore, the resulting microstructures would vary between them. Different microstructures result in different combustion velocities because parameters such as laminate size, laminate frequency, defect density, and inter-particle porosity will change as the milling parameters are changed.[11,24,27] All of these factors play a role in the resulting combustion velocities of these materials.

D. Thermal analysis

DSC analysis of the MA Ni/Al material dry milled for 25% t_{cr} and 97% t_{cr} indicates that in the temperature range of 450 K to 850 K, the materials react and exhibit three exothermic peaks before the melting point of Al.[10] DSC analysis of material dry milled for 50% t_{cr} and 75% t_{cr} show the same trend (see Fig. 6). As the milling time increases, the reaction onset temperatures and exothermic peaks shift to lower temperatures by 25–80 K as compared with material dry milled for 25% t_{cr}. Previous work has shown that the decrease in sensitivity to thermal and mechanical impact is largely dictated by the temperature needed to begin the initial exothermic reaction (peak A).[10,24,25] The exothermic reaction of peak A is due to the release of stored free energy and initial dissolution of nickel into aluminum,[10,23,27] where the stored free energy is acquired by the formation of microdeformations (vacancies and dislocations) and amorphous Al during the milling process.[23,27,28] It is largely due to the introduction and increase in concentration of these components that results in the decrease of temperature needed to initiate the Ni/Al reaction.[27] Recent work has shown the initial formation of microdeformations and amorphous Al can occur at milling times starting at about 15% t_{cr}.[27] This is supported with these DSC results and thermal ignition experiments[10] as ignition temperatures are significantly less than typical Ni/Al

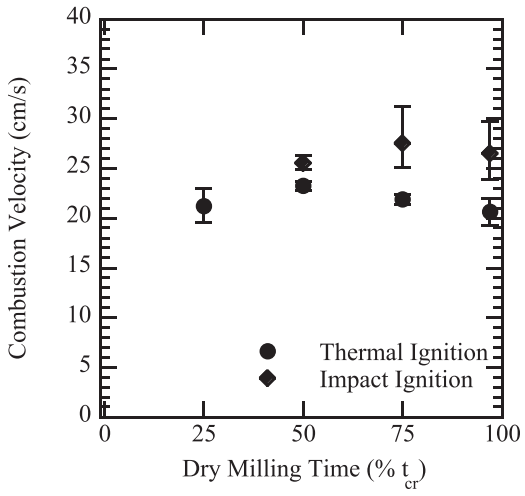

FIG. 5. Average combustion velocity of MA Ni/Al samples thermally ignited and impacted with an impact energy of 200–250 J (130–140 m/s).

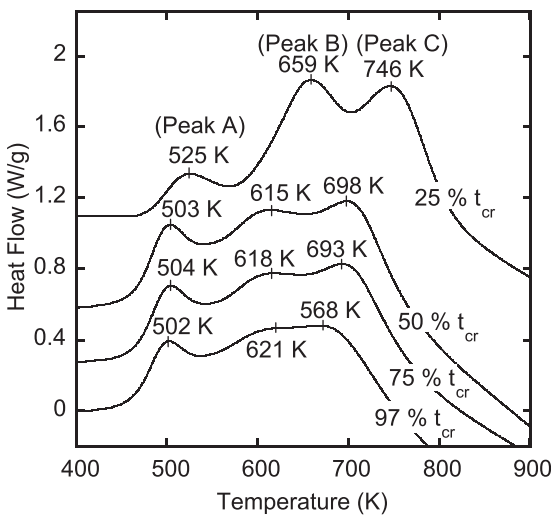

FIG. 6. DSC traces for MA Ni/Al as a function of milling time.

ignition temperatures (~913 K). However, the lower temperature needed to initiate the initial exothermic reaction (peak A) reaches a minimum at a milling time of 50% t_{cr}. It is also at this milling duration that the initial formation of nanolaminate structures is detected.

As shown in Table II, the exothermic reaction onset temperature for peak A is about 479 K for a dry milling time of 25% t_{cr} and then it lowers to about 460 K and does not change significantly for dry milling times $\geq$ 50% t_{cr}. In addition to the reaction onset temperature, it is also between the milling times of 25% t_{cr} and 50% t_{cr} that the thermal ignition threshold lowers from about 660 K to 590 K and the mechanical impact ignition threshold lowers from an impact energy of greater than 500 J (200 m/s) to about 200 J (130 m/s). The increase reaction sensitivity between the milling times of 25% t_{cr} and 50% t_{cr} is likely due to a combination of increases in the concentration of microdeformations, amorphous Al and to the initial formation of nanolaminate structures in the MA Ni/Al material. Further milling beyond 50% t_{cr} continues to increase the fraction of nanolaminate material and the thermal and impact ignition thresholds also decrease, however to a lesser extent.

With the decrease in thermal ignition temperatures, there is also a loss in energy, the heat of reaction for the combined reaction of peaks B and C changes significantly as a function of milling time (see Table II). Between the milling times of 25% t_{cr} and 50% t_{cr}, the heat of reaction for the combined reaction of peaks B and C decreases significantly from 515 J/g to 154 J/g, respectively. As the dry milling time is increased from 50% t_{cr} to 97% t_{cr}, the magnitude and peak temperature of peak B remains unchanged but the 3rd peak continues to shift to a lower temperature while its magnitude decreases resulting in a slightly lower heat of reaction for the combined reaction (peaks B and C). This indicates that an optimum milling time could be found where the sensitivity to thermal and mechanical impact is greatly increased and the loss of energy due to increased milling is minimized. For this system and milling method, the optimum dry milling time is in the range 50%–75% t_{cr}.

This loss in energy in peaks B and C is potentially caused by the formation of intermediate Al/Ni phases formed during milling, however, different phases were not detected in unreacted material for any of the dry milling times considered,[10] which could indicate the presence of amorphous intermediate Al/Ni phases or solid solutions. Further XRD analysis of samples annealed to 690 K (dry milling time of 25% t_{cr}) or 620 K (dry milling times of 50% t_{cr} to 97% t_{cr}) show that the dominate phases present just after the reaction of Peak B are Ni, Al_3Ni, and Al_3Ni_2 regardless of the milling time. It has previously been shown that material annealed to just after peak C (770 K) consist only of the phases Ni, Al_3Ni_2, and NiAl and material annealed to 1070 K consisted of mainly NiAl regardless of whether the material dry milled for 25% t_{cr} or 97% t_{cr}.

TABLE II. Reaction onset temperatures and heat of formation for acquired DSC traces.

	Peak A		Peak B-C	
Dry milling time (% t_{cr})	Onset temperature (K)	Heat of reaction (J/g)	Onset temperature (K)	Heat of reaction (J/g)
25	479	41	592	515
50	463	52	558	154
75	463	54	558	153
97	461	46	552	117

IV. SUMMARY AND CONCLUSIONS

In summary, our experiments show that refining the microstructure of MA Ni/Al reactive composites by varying the dry milling time significantly affects the mechanical impact ignition threshold and resulting combustion behavior. For dry milling times of 0%–25% t_{cr}, the impact ignition thresholds are greater than at least 500 J (200 m/s); and as the milling time increases to 50% t_{cr}, the impact ignition threshold reduces to ~200 J (130 m/s). Further milling reduces the impact ignition threshold to ~40–60 J (60–70 m/s) as the total dry milling time increases from 50% t_{cr} to 97% t_{cr}. High velocity imaging also showed that ignition of the sample occurred at ignition spots typically on or near the impact face and edges of the sample. Ignition delays were found to be on the order of 1–6.5 ms and combustion velocities were on the order of 25–31 cm/s. Increased milling had little effect on the ignition delays or combustion velocities as long as the material was dry milled to at least 50% t_{cr}. Combustion velocities for compacts that were thermally ignited were in the range of 21–23 cm/s for milling times of 25–75% t_{cr}, while unmilled materials did not propagate unless preheated for the densities considered.

These results along with DSC analysis indicate that (i) the driving mechanism behind reaction upon impact for these experiments is the rapid increase in temperature at localized hot spots on or near the impact face and edges of the sample and that when the hotspots reach the thermal ignition threshold, the impacted sample ignites and (ii) that although increasing the milling time to near the critical milling time may reduce the thermal and impact ignition thresholds, the reductions are modest beyond a point and may not be worth the loss in reaction energy due to further milling. Here, we find that the largest jump in sensitivity is between the dry milling times of 25% t_{cr} and 50% t_{cr} corresponding to when nanolaminate structures are initially detected during the ball milling process. Thermal analysis along with previous work indicates that the increase in the sensitivity to thermal and mechanical impact is dictated by a combination of three coupled factors: the formation of microdeformations (vacancies and dislocations), amorphous Al, and nanolaminate structures, which reduce the temperature needed to begin the dissolution of nickel into aluminum. DSC analysis showed that between the dry milling times of 25% t_{cr} and 50% t_{cr}, the onset of the dissolution of nickel into aluminum shifted from 479 K to 462 K. Further dry milling of the MA Ni/Al does not reduce the onset of the dissolution of nickel into aluminum but it does reduce the total energy output of the system, indicating that for this system and method, a milling time

of about 50%–75% t_{cr} is likely optimal when taking into account both the increased ignition sensitively of mechanical activation and potential loss in reaction energy with longer milling times.

With these results, a more comprehensive understanding of how MA affects the impact and reaction behavior of MA Ni/Al is achieved that can aid in the modeling of these systems and in their application.

ACKNOWLEDGMENTS

Funding from the Defense Threat Reduction Agency (DTRA), Grant No. HDTRA1-10-1-0119 Counter-WMD basic research program, Dr. Suhithi M. Peiris, program director is gratefully acknowledged. Additional funding and support was provided by the William K. and Gail E. Cordier Fellowship. The Authors would like to acknowledge Dr. Khachatur Manukyan and Professor Alexander Mukasyan of Notre Dame University for performing XRD analysis. Authors would also like to acknowledge the suggestions and encouragement of Professor Alejandro Strachan of Purdue University.

[1]D. E. Eakins and N. N. Thadhani, Int. Mater. Rev. **54**, 181 (2009).
[2]E. M. Hunt and M. L. Pantoya, Intermetallics **18**, 1612 (2010).
[3]X. F. Zhang, A. S. Shi, J. Zhang, L. Qiao, Y. He, and Z. W. Guan, J. Appl. Phys. **111**, 123501 (2012).
[4]A. Bacciochini, M. I. Radulescu, Y. Charron-Tousignant, J. Van Dyke, M. Nganbe, M. Yandouzi, J. J. Lee, and B. Jodoin, Surf. Coat. Technol. **206**, 4343 (2012).
[5]E. B. Herbold, N. N. Thadhani, and J. L. Jordan, J. Appl. Phys. **109**, 066108 (2011).
[6]N. N. Thadhani, J. Appl. Phys. **76**, 2129 (1994).
[7]S. W. Du and N. N. Thadhani, AIP Conf. Proc. **1195**, 470 (2009).
[8]E. M. Hunt, K. B. Plantier, and M. L. Pantoya, Acta Mater. **52**, 3183 (2004).
[9]R. V. Reeves, A. S. Mukasyan, and S. F. Son, J. Phys. Chem. C **114**, 14772 (2010).
[10]K. V. Manukyan, B. A. Mason, L. J. Groven, Y. C. Lin, M. Cherukara, S. F. Son, A. Strachan, and A. S. Mukasyan, J. Phys. Chem. C **116**, 21027 (2012).
[11]E. B. Herbold, J. L. Jordan, and N. N. Thadhani, Acta Mater. **59**, 6717 (2011).
[12]R. V. Reeves, A. S. Mukasyan, and S. F. Son, in *Shock Compression of Condensed Matter—2011, Pts 1 and 2*, edited by M. L. Elert, W. T. Buttler, J. P. Borg, J. L. Jordan, and T. J. Vogler (Amercian Institute of Physics, Melville, 2012), Vol. 1426, p. 539.
[13]A. Hadjiafxenti, I. E. Gunduz, C. Tsotsos, T. Kyratsi, S. M. Aouadi, C. C. Doumanidis, and C. Rebholz, J. Alloys Compd. **505**, 467 (2010).
[14]A. Hadjiafxenti, I. E. Gunduz, C. Tsotsos, T. Kyratsi, C. C. Doumanidis, and C. Rebholz, Intermetallics **18**, 2219 (2010).
[15]A. R. Nair, B. A. Mason, L. J. Groven, S. F. Son, A. Strachan, and A. M. Cuitiño, "Micro-RVE modeling of mechanistic response in porous intermetallics subject to weak and moderate impact loading," Inter'l. J. Plasticity (published online).
[16]M. J. Cherukara, K. G. Vishnu, and A. Strachan, Phys. Rev. B **86**, 075470 (2012).
[17]B. W. Asay, D. J. Funk, C. S. Fugard, P. M. Dickson, and B. F. Henson, AIP Conf. Proc. **429**, 567 (1997).
[18]R. V. Reeves, J. D. E. White, A. M. Mukasyan, and S. F. Son, in *Shock Compression of Condensed Matter—2009, Pts 1 and 2*, edited by M. L. Elert, W. T. Buttler, M. D. Furnish, W. W. Anderson, and W. G. Proud (2009), Vol. 1195, p. 466.
[19]L. Thiers, A. S. Mukasyan, and A. Varma, Combust. Flame **131**, 198 (2002).
[20]A. Biswas and S. K. Roy, Acta Mater. **52**, 257 (2004).
[21]K. Morsi, Mater. Sci. Eng., A **299**, 1 (2001).
[22]P. Zhu, J. C. M. Li, and C. T. Liu, Mater. Sci. Eng. A **329**, 57 (2002).
[23]M. A. Korchagin, T. F. Grigor'eva, B. B. Bokhonov, M. R. Sharafutdinov, A. P. Barinova, and N. Z. Lyakhov, Combust. Explos. Shock Waves **39**, 43 (2003).
[24]C. Suryanarayana, Prog. Mater. Sci. **46**, 1 (2001).
[25]V. M. Maslov, I. P. Borovinskaya, and A. G. Merzhanov, Combust. Explos. Shock Waves **12**, 631 (1976).
[26]Y. S. Naiborodenko and V. I. Itin, Combust. Explos. Shock Waves **11**, 293 (1975).
[27]D. Y. Kovalev, N. A. Kochetov, and V. I. Ponomarev, Combust. Explos. Shock Waves **46**, 457 (2010).
[28]M. A. Korchagin, T. F. Grigor'eva, B. B. Bokhonov, M. R. Sharafutdinov, A. P. Barinova, and N. Z. Lyakhov, Combust. Explos. Shock Waves **39**, 51 (2003).